

---

# A functional mirror ascent view of policy gradient methods with function approximation

---

**Sharan Vaswani** <sup>\*</sup>  
Amii, University of Alberta

**Olivier Bachem**  
Google Brain

**Simone Totaro**  
Mila, Université de Montréal

**Robert Müller**  
TU Munich

**Matthieu Geist**  
Google Brain

**Marlos C. Machado**<sup>†</sup>  
Amii, University of Alberta  
DeepMind

**Pablo Samuel Castro**  
Google Brain

**Nicolas Le Roux**<sup>†</sup>  
Mila, Université de Montréal  
McGill University

## Abstract

We use functional mirror ascent to propose a general framework (referred to as FMA-PG) for designing policy gradient methods. The functional perspective distinguishes between a policy’s functional representation (what are its sufficient statistics) and its parameterization (how are these statistics represented), and naturally results in computationally efficient off-policy updates. For simple policy parameterizations, the FMA-PG framework ensures that the optimal policy is a fixed point of the updates. It also allows us to handle complex policy parameterizations (e.g., neural networks) while guaranteeing policy improvement. Our framework unifies several PG methods and opens the way for designing sample-efficient variants of existing methods. Moreover, it recovers important implementation heuristics (e.g., using forward vs reverse KL divergence) in a principled way. With a softmax functional representation, FMA-PG results in a variant of TRPO with additional desirable properties. It also suggests an improved variant of PPO, whose robustness and efficiency we empirically demonstrate on MuJoCo. Via experiments on simple reinforcement learning problems, we evaluate algorithms instantiated by FMA-PG.

## 1 Introduction

Policy gradient (PG) methods [36, 32, 19, 17] are an important class of model-free methods in reinforcement learning. They allow for a differentiable policy parameterization, and can easily handle function approximation and structured state-action spaces. PG methods based on REINFORCE [37] are equipped with strong theoretical guarantees in restricted settings [2, 24, 7]. For these methods, each policy update requires recomputing the policy gradient. This in turn requires interacting with the environment or the simulator which can be computationally expensive. On the other hand, methods such as TRPO [27], PPO [28] and MPO [1] support “off-policy updates” i.e. they can update the policy without requiring additional interactions with the environment. These methods are efficiently implementable, have good empirical performance [8] and are commonly used in deep reinforcement learning [10]. However, they only have weak theoretical guarantees in the tabular setting [16, 27, 25, 11, 29]. Consequently, there are numerous discrepancies between the theory and

---

<sup>\*</sup>Correspondence to vaswani.sharan@gmail.com

<sup>†</sup>Canada CIFAR AI Chair

practice of these methods [21, 23, 9]. Most importantly, there is no principled way to design such PG methods or a unified framework to analyze their theoretical properties.

To address these issues, we view PG methods through the lens of a functional mirror ascent framework. This viewpoint distinguishes between a policy’s functional representation (its sufficient statistics) such as the conditional distribution over actions given states or the induced stationary distribution; and its parameterization (how are these statistics represented) such as a linear model or deep network. Our framework unifies different perspectives and provides a principled way to develop and analyze computationally efficient PG methods. In particular, we make the following contributions.

**Functional mirror ascent for policy gradient:** In Section 2, we first give examples to distinguish between a policy’s functional representation and its parameterization. In Section 3, we specify the functional mirror ascent (FMA) update and connect it to policy gradient methods. In particular, we show that FMA can be interpreted as the repeated application of a policy improvement and a projection (onto the set of feasible policies) operator [12]. For simple policy parameterizations, we prove that the FMA updates are consistent [12] ensuring that the optimal policy (in the class) is a fixed point of the resulting PG method.

**Instantiating the FMA framework:** In Section 4, we instantiate the general FMA framework with two common functional representations – direct and softmax representations. In the tabular setting with finite states and actions, we show that the resulting FMA updates recover conservative policy iteration [16] and REINFORCE-based methods analyzed in [2, 24, 7].

**Generic policy gradient framework:** In Section 5, we propose a reparameterization technique to handle arbitrarily complex policy parameterizations. This results in FMA-PG, a generic policy gradient framework based on FMA. FMA-PG naturally results in computationally efficient off-policy updates and is instantiated by choosing a functional representation and a policy parameterization. When instantiated with the softmax functional representation, FMA-PG results in an improved, more stable variant of TRPO [27] and MDPO [34]. Moreover, it recovers implementation heuristics (e.g. using forward vs reverse KL divergence) in a principled manner. In addition, in Appendix A, we show that the FMA-PG framework can handle stochastic value gradients [13].

**Theoretical guarantees:** In Section 6, we give a principled way to set the FMA step-size for the direct and softmax representations. With appropriate step-sizes, the FMA-PG updates are guaranteed to improve the policy and converge to a stationary point for *any arbitrary policy parameterization*.

**Experimental evaluation:** Finally, in Section 7, we evaluate variants of FMA-PG for simple bandit and reinforcement learning settings. FMA-PG also suggests a variant of PPO [28], whose robustness and efficiency we demonstrate on continuous control tasks in the MuJoco environment [33].

## 2 Problem Formulation

We consider an infinite-horizon discounted Markov decision process (MDP) [26] defined by the tuple  $\mathcal{M} = \langle \mathcal{S}, \mathcal{A}, p, r, d_0, \gamma \rangle$  where  $\mathcal{S}$  is a potentially infinite set of states,  $\mathcal{A}$  is a potentially infinite action set,  $p : \mathcal{S} \times \mathcal{A} \rightarrow \Delta^{\mathcal{S}}$  is the transition probability function,  $r : \mathcal{S} \times \mathcal{A} \rightarrow \mathbb{R}$  is the reward function,  $d_0$  is the initial distribution of states, and  $\gamma \in [0, 1)$  is the discount factor.

Throughout this paper, we distinguish a policy’s functional representation from its parameterization. We will use  $\pi$  to denote the *functional representation* of the corresponding policy. A policy’s functional representation defines its sufficient statistics and can be non-parametric. For example, we may define a policy via a distribution  $p^{\pi}(\cdot|s)$  over the actions for each state  $s \in \mathcal{S}$ , which we call the *direct representation*. Such a representation is used for stochastic policies typically used with policy gradient algorithms [31]. Since  $p^{\pi}(\cdot|s)$  is a probability distribution, an equivalent form is the *softmax representation*  $p^{\pi}(a|s) = \exp(z^{\pi}(a, s)) / \sum_a \exp(z^{\pi}(a', s))$  where the policy is specified by the  $z^{\pi}(a, s)$  variables. Note that though the direct and softmax representations are equivalent in the class of policies they define, they result in different functional updates (Sections 4.1 and 4.2), and thus different algorithms. Alternatively, one can specify a stochastic policy by its state-occupancy measures [26] or represent a deterministic, stationary policy by specifying the state-action mapping for each state. The functional representation affects the final algorithm but it is never made explicit.

Regardless of its representation, each policy  $\pi$  induces a distribution  $p^{\pi}(\cdot|s)$  over actions for each state  $s$ . It also induces a measure  $d^{\pi}$  over states such that  $d^{\pi}(s) = \sum_{t=0}^{\infty} \gamma^t \mathbb{P}(s_{t+1} = s \mid s_0 \sim$

$d_0, a_t \sim p^\pi(a_t|s_t)$ . Similarly we define  $\mu^\pi$  as the unnormalized distribution over state-action pairs induced by policy  $\pi$ , implying that  $\mu^\pi(s, a) = d^\pi(s)p^\pi(a|s)$  and  $d^\pi(s) = \sum_a \mu^\pi(s, a)$ . The expected discounted return for  $\pi$  is defined as  $J(\pi) = \mathbb{E}_{s_0, a_0, \dots} \left[ \sum_{t=0}^{\infty} \gamma^t r(s_t, a_t) \right]$ , where  $s_0 \sim d_0$ ,  $a_t \sim p^\pi(a_t|s_t)$ , and  $s_{t+1} \sim p(s_{t+1}|s_t, a_t)$ . Given a policy representation, the agent's objective is to learn the policy that maximizes the expected discounted return.

While the functional representation defines a policy's sufficient statistics, the parameterization specifies the practical realization of these statistics. The policy parameterization is independent of its functional representation, it is explicit and determined by a model whose parameters  $\theta$  are optimized by a policy gradient algorithm. For example, we could represent a policy by its state-action occupancy measure and use a linear parameterization to define this measure, implying  $\mu^\pi(s, a|\theta) = \langle \theta, \phi(s, a) \rangle$ , where  $\theta$  is the parameter to be optimized and  $\phi(s, a)$  are the known features providing information about the state-occupancy measures. Similarly, we could use a neural-network parameterization for the variables that define a policy in its softmax representation, rewriting  $z^\pi(a, s) = z^\pi(a, s|\theta)$ . The *tabular parameterization* is special and makes the functional representation of a policy equivalent to its parameterization. For a finite state-action MDP with  $S$  states and  $A$  actions, choosing a tabular parameterization with the softmax representation results in  $\theta \in \mathbb{R}^{SA}$  such that  $\forall s \in \mathcal{S}, a \in \mathcal{A}$ ,  $z^\pi(a, s|\theta) = \theta_{s,a}$ . The tabular parameterization is studied in previous work [2, 24]. The policy parameterization defines the set  $\Pi$  of realizable (representable) policies. For example, when using the direct functional representation with a tabular parameterization, the set  $\Pi$  is a simplex. We denote by  $\pi^* := \arg \max_{\pi \in \Pi} J(\pi)$  as the *optimal policy* in the class. In the next section, we describe the functional mirror ascent framework and how to design a generic policy gradient method.

### 3 Functional mirror ascent framework

In this section, we first give the FMA update and explain how it can be used to define a pair of consistent operators that ensure  $\pi^*$  is a fixed point.

To specify the functional mirror ascent (FMA) update, we define a strictly convex, differentiable function  $\phi$  as the mirror map. We denote by  $D_\phi(\pi, \mu)$  the Bregman divergence associated with the mirror map  $\phi$  between policies  $\pi$  and  $\mu$ . Each iteration  $t \in [T]$  of FMA consists of the update and projection steps [6]: Eq. (1) computes the gradient  $\nabla_\pi J(\pi_t)$  with respect to the policy's functional representation and updates  $\pi_t$  to  $\pi_{t+1/2}$  using a step-size  $\eta$ ; Eq. (2) computes the Bregman projection of  $\pi_{t+1/2}$  onto the class of realizable policies, obtaining  $\pi_{t+1}$ .

$$\pi_{t+1/2} = (\nabla \phi)^{-1} (\nabla \phi(\pi_t) + \eta \nabla J(\pi_t)), \quad (1)$$

$$\pi_{t+1} = \arg \min_{\pi \in \Pi} D_\phi(\pi, \pi_{t+1/2}). \quad (2)$$

The above FMA updates can also be written as [c.f. 6]:

$$\pi_{t+1} = \arg \max_{\pi \in \Pi} \left[ \langle \pi, \nabla_\pi J(\pi_t) \rangle - \frac{1}{\eta} D_\phi(\pi, \pi_t) \right]. \quad (3)$$

Note that the FMA update is solely in the functional space and requires solving the above projection as a sub-problem. The policy parameterization defines the set  $\Pi$  of realizable policies and influences the difficulty of solving Eq. (3). We now connect the FMA update to policy gradient and explain the conditions under which  $\pi^*$  is its fixed point.

#### 3.1 Connecting FMA to policy gradient

Several iterative PG methods can be viewed as the repeated application of the *improvement* and *projection* operators [12]. Specifically, at iteration  $t$  of a PG method:

1. An improvement operator  $\mathcal{I}$  transforms the current policy  $\pi_t$  into an improved policy  $\pi_{t+1/2} = \mathcal{I}\pi_t$ . The improvement operator guarantees a higher expected return, implying that  $J(\pi_{t+1/2}) \geq J(\pi_t)$ . However, the policy  $\pi_{t+1/2}$  might be outside of the policy class  $\Pi$ .
2. The projection operator  $\mathcal{P}$  projects  $\pi_{t+1/2}$  onto set  $\Pi$  to yield  $\pi_{t+1} = \mathcal{P}\pi_{t+1/2} = \mathcal{P} \circ \mathcal{I}\pi_t$ .

Ghosh et al. [12] introduced the notion of *consistency* of a pair of operators  $(\mathcal{I}, \mathcal{P})$  to mean that  $\pi^*$  is a fixed point of  $\mathcal{P} \circ \mathcal{I}$ . They showed that the corresponding operators for REINFORCE form a

consistent pair in the tabular setting. However, the corresponding operators for both PPO and MPO, two commonly used PG methods, do not form a consistent pair. This implies that these methods are not guaranteed to converge to the optimal policy even in the tabular setting.

Using a pair of consistent operators is a necessary but not a sufficient condition for convergence to the optimal policy. In this paper, we associate the pair  $(\mathcal{I}, \mathcal{P})$  of operators with the update and projection steps of the functional mirror descent step. Specifically, we define the operators  $\tilde{\mathcal{I}}$  and  $\mathcal{P}$  such that, at iteration  $t$ ,  $\mathcal{I}\pi_t := \pi_{t+1/2}$  (Eq. (1)) and  $\mathcal{P} \circ \tilde{\mathcal{I}}\pi_t := \mathcal{P}\pi_{t+1/2} = \pi_{t+1}$  (Eq. (2)). *We now show that this choice always results in pairs of consistent operators.*

**Proposition 1** (Operator consistency for the FMA update). *By defining the improvement and projection operators as the update and projection step of FMA, for the same mirror map (as in Eqs. (1) and (2)),  $\pi^*$  is a fixed point of  $\mathcal{P} \circ \mathcal{I}$ .*

Note that the proof of the above proposition relies on exactly solving the minimization step in Eq. (2). When using the tabular or linear parameterization, the set  $\Pi$  of realizable policies is convex and, since the function  $D_\phi(\cdot, \pi)$  is convex for all  $\pi$ , the minimization can be done exactly. In this case, Proposition 1 implies that the optimal policy  $\pi^*$  is a fixed point (of many) of the FMA update.

In the next section, we instantiate this framework with two commonly used functional representations.

## 4 Instantiating the FMA framework

We use FMA with two common functional representations – the direct representation (Section 4.1) and the softmax representation (Section 4.2). In this section, we only consider the functional aspect and the tabular parameterization, while in Section 5 we handle general policy parameterization and projections onto  $\Pi$ .

### 4.1 Direct functional representation

In the direct functional representation, the policy  $\pi$  is represented by the set of distributions  $p^\pi(\cdot|s)$  over actions for each state  $s \in \mathcal{S}$ . In this case,  $\frac{\partial J(\pi)}{\partial p^\pi(a|s)} = d^\pi(s)Q^\pi(s, a)$ . Since  $p^\pi(\cdot|s)$  is a set of distributions, we define the mirror map as  $\phi(\pi) = \sum_{s \in \mathcal{S}} w(s) \phi(p^\pi(\cdot|s))$ , where  $w(s)$  is any positive weighting on the states  $s$ . Note that the positive weights ensure that  $\phi(\pi)$  is a valid mirror-map. The resulting Bregman divergence is  $D_\phi(\pi, \pi') = \sum_s w(s)D_\phi(p^\pi(\cdot|s), p^{\pi'}(\cdot|s))$ , that is, the weighted sum of the Bregman divergences between the action distributions in state  $s$ . By choosing  $w(s)$  equal to  $d^{\pi_t}(s)$ , Eq. (3) becomes

$$\pi_{t+1} = \arg \max_{\pi \in \Pi} \mathbb{E}_{(s, a) \sim \mu^{\pi_t}} \left[ \left( Q^{\pi_t}(s, a) \frac{p^\pi(a|s)}{p^{\pi_t}(a|s)} \right) - \frac{1}{\eta} D_\phi(p^\pi(\cdot|s), p^{\pi_t}(\cdot|s)) \right]. \quad (4)$$

When instantiated with the direct functional representation and a tabular parameterization, the FMA update recovers existing PG methods.

**Connection to CPI:** The first term of Eq. (4) is the standard linearization of the loss in the functional space. For finite states and actions, using a tabular parameterization results in an equivalence between the functional and parametric spaces and the first term becomes the same as in conservative policy iteration (CPI) [16]. In CPI, the authors first derive the form  $\sum_s d^\pi(s) \sum_a p^\pi(a|s) Q^{\pi_t}(s, a)$ , then use a mixture policy to ensure that  $\pi$  is “close” to  $\pi_t$  and justify replacing  $d^\pi(s)$  in the above expression by  $d^{\pi_t}$ . On the other hand, we use the FMA update to directly derive Eq. (4) and allow for the use of any Bregman divergence to ensure the proximity between  $\pi$  and  $\pi_t$ .

**Connection to REINFORCE-based methods and TPRO:** For finite states and actions, and a tabular parameterization, the feasible set  $\Pi$  is the  $SA$ -dimensional simplex. In this case, if we choose the squared Euclidean distance as the mirror map, Eq. (4) is the same as the standard REINFORCE update [37, 2]. Choosing the negative entropy as the mirror map results in a Bregman divergence equal to the KL divergence. With this choice and a tabular parameterization, Eq. (4) is equal to the natural policy gradient update [15, 18]. It is also similar to the update in uniform TRPO [29] and Mirror Descent Modified Policy Iteration [11].

Since  $p^\pi(\cdot|s)$  is a distribution, it has an equivalent softmax representation which we study next.

---

**Algorithm 1:** FMA-PG: Generic algorithm for policy optimization

---

**Input:**  $\pi_0$  (initial policy),  $T$  (PG iterations),  $m$  (inner-loops),  $\eta$  (Step-size for functional update),  $\alpha$  (Step-size for parametric update)

**for**  $t \leftarrow 0$  **to**  $T - 1$  **do**

Compute gradient  $\nabla_{\pi} J(\pi_t)$  and form function  $\ell_t^{\pi, \phi, \eta}(\theta)$  as in Eq. (8)

Initialize inner-loop:  $\omega_0 = \theta_t$

**for**  $k \leftarrow 0$  **to**  $m$  **do**

$\omega_{k+1} = \omega_k + \alpha \nabla_{\omega} \ell_t^{\pi, \phi, \eta}(\omega_k)$

**end**

$\theta_{t+1} = \omega_m$

$\pi_{t+1} = \pi(\theta_{t+1})$

**end**

Return  $\theta_T$

---

## 4.2 Softmax functional representation

The softmax functional representation results in the FMA update on the logits  $z^{\pi}(a, s)$  of the conditional distributions  $p^{\pi}(a|s)$ . Formally,  $p^{\pi}(a|s) = \frac{\exp(z^{\pi}(a, s))}{\sum_{a'} \exp(z^{\pi}(a', s))}$  and the policy gradient theorem yields  $\frac{\partial J(\pi)}{\partial z^{\pi}(a, s)} = d^{\pi}(s) A^{\pi}(s, a) p^{\pi}(a|s)$ . Here,  $A^{\pi}(s, a)$  is the advantage function equal to  $Q^{\pi}(s, a) - V^{\pi}(s)$ . Similar to Section 4.1, we use a mirror map  $\phi_z(z)$  that decomposes across states, i.e.  $\phi_z(z) = \sum_s w(s) \phi_z(z^{\pi}(\cdot, s))$  for some positive weighting  $w$ . We denote the corresponding Bregman divergence as  $D_{\phi_z}$ . Using  $w(s) = d^{\pi_t}(s)$ , Eq. (3) becomes equal to

$$\pi_{t+1} = \arg \max_{\Pi} E_{(s, a) \sim \mu^{\pi_t}} \left[ A^{\pi_t}(s, a) p^{\pi_t}(a|s) - \frac{1}{\eta} \sum_s w(s) D_{\phi_z}(z^{\pi}(\cdot, s), z^{\pi_t}(\cdot, s)) \right]. \quad (5)$$

**Connection to REINFORCE-based methods:** For finite states and actions, using a tabular parameterization and the squared Euclidean mirror map, the update in Eq. (5) becomes equal to that of policy gradient with the softmax parameterization [2, 24]. In the tabular setting, the results in these papers suggest that the softmax parameterization leads to faster convergence than the direct parameterization.

A possible choice for  $\phi$  is the normalized exponential, i.e.  $\phi_z(z) = \sum_s w(s) \frac{\sum_a \exp(z^{\pi}(a, s))}{\sum_a \exp(z^{\pi_t}(a, s))}$ . By using  $w(s) = d^{\pi_t}(s)$ , solving Eq. (5) is equivalent to solving

$$\pi_{t+1} = \arg \max_{\pi \in \Pi} E_{(s, a) \sim \mu^{\pi_t}} \left[ \left( A^{\pi_t}(s, a) + \frac{1}{\eta} \right) \log \frac{p^{\pi}(a|s)}{p^{\pi_t}(a|s)} \right]. \quad (6)$$

The full derivation of this computation can be found in Proposition 4 of Appendix C. Notice that unlike Eq. (4), Eq. (6) only involves the logarithm of the importance sampling ratio  $p^{\pi}(a|s)/p^{\pi_t}(a|s)$ . This difference will result in more stable off-policy updates in Section 5.

**Tabular parameterization:** In the finite state-action case with tabular parameterization, the objective in Eq. (6) can be maximized analytically to yield  $p^{\pi_{t+1}}(a|s) \propto p^{\pi_t}(a|s) \max(1 + \eta A^{\pi_t}(s, a), 0)$ .

Both updates in Eqs. (4) and (6) involve a projection onto the class of feasible policies  $\Pi$  and require specifying  $\eta$ . In the next section, we handle the projection step for arbitrary policy parameterizations and discuss the choice of  $\eta$  in Section 6.

## 5 Policy parameterization

As explained earlier, the class  $\Pi$  of realizable policies is determined by the policy parameterization. For simple parameterizations such as tabular, the set  $\Pi$  is convex and the minimization in Eq. (3) can be done exactly. When using more complex policy parameterizations (e.g. deep neural network), the set of realizable policies  $\Pi$  can become arbitrarily complicated and non-convex, making the projection in Eq. (3) infeasible. Instead, to handle arbitrary policy parameterizations, we reparameterize the constrained optimization in Eq. (3) as an unconstrained optimization problem. We assume that  $\Pi$  consists of policies that are realizable by a model parameterized by  $\theta \in \mathbb{R}^d$ . Throughout the remaining

paper, we will continue to use  $\pi$  to refer to a policy's functional representation whereas  $\pi(\theta)$  will refer to the parametric realization of  $\pi$ . Note that any generic model (e.g. neural network) can be used to parameterize  $\pi$  and is implicit in the  $\pi(\theta)$  notation. For the special case of the tabular parameterization,  $\pi = \pi(\theta) = \theta$ . Using the above definition, the following two problems are equivalent:

$$\max_{\pi \in \Pi} J(\pi) = \max_{\theta \in \mathbb{R}^d} J(\pi(\theta)) . \quad (7)$$

With this reparameterization, no projection is required and the update in Eq. (3) can be written as a parametric, unconstrained optimization problem, with  $\pi_t = \pi(\theta_t)$  and  $\pi_{t+1} = \pi(\theta_{t+1})$ ,

$$\theta_{t+1} = \arg \max_{\theta \in \mathbb{R}^d} \left[ \underbrace{J(\pi(\theta_t)) + \langle \pi(\theta) - \pi(\theta_t), \nabla_{\pi} J(\pi(\theta_t)) \rangle - \frac{1}{\eta} D_{\phi}(\pi(\theta), \pi(\theta_t))}_{:= \ell_t^{\pi, \phi, \eta}(\theta)} \right] , \quad (8)$$

where  $\ell_t^{\pi, \phi, \eta}$  respectively denotes the dependence of the objective on the functional representation, the mirror map, and  $\eta$ . Note that, compared to Eq. (3), we added terms independent of  $\theta$  which do not change the arg max but will prove useful in Section 6. The objective in Eq. (8) is non-concave in general and can be maximized using a gradient-based algorithm. We will use  $m$  gradient steps with a step-size  $\alpha$  to maximize  $\ell_t^{\pi, \phi, \eta}(\theta)$ .

The overall algorithm is referred to as FMA-PG and its pseudo-code is given in Algorithm 1. Observe that the policy's functional representation affects the gradient  $\nabla_{\pi} J(\pi_t)$ . It is used to form the function  $\ell_t^{\pi, \phi, \eta}$  that acts as a “guide” for the parametric updates in the inner-loop, similar to the algorithm proposed for supervised learning by Johnson and Zhang [14]. FMA-PG can be used with any functional representation or policy parameterization. We now consider the special case of the direct and softmax function representations and derive the corresponding  $\ell_t^{\pi, \phi, \eta}$  functions.

Specifically, we parameterize the direct functional representation as  $p^{\pi}(\cdot|s, \theta)$  in Eq. (4). Noting that  $p^{\pi_t}(\cdot|s) = p^{\pi}(\cdot|s, \theta_t)$ , we obtain the following form of  $\ell_t^{\pi, \phi, \eta}$ :

$$\ell_t^{\pi, \phi, \eta}(\theta) = \mathbb{E}_{(s, a) \sim \mu^{\pi_t}} \left[ \left( Q^{\pi_t}(s, a) \frac{p^{\pi}(a|s, \theta)}{p^{\pi}(a|s, \theta_t)} \right) - \frac{1}{\eta} D_{\phi}(p^{\pi}(\cdot|s, \theta), p^{\pi}(\cdot|s, \theta_t)) \right] + C , \quad (9)$$

with  $C$  a constant independent of  $\theta$ . Eq. (9) shows the benefits of first casting policy gradient methods as functional mirror ascent, and then using parametric updates to solve the resulting projection subproblem. If we had directly chosen a parameterization and optimized  $J(\pi(\theta))$  over  $\theta$ , each parametric update would require computing the gradient and consequently involve collecting samples from the current policy  $\pi(\theta_t)$ . This aspect of the PG methods analyzed in [2, 23] makes them computationally expensive. Note that these methods can be obtained by using FMA-PG with  $m = 1$ .

On the other hand, FMA-PG with multiple steps,  $m > 1$ , requires parametric updates for optimizing the expression in Eq. (9). These updates rely on the states sampled from the fixed policy  $\pi_t$ . This natural *off-policyness* is an important feature of commonly used PG methods such as TRPO [27], PPO [28] and enable policy updates without interacting with the environment.

**Comparison to MDPO:** With a direct functional representation and the negative entropy as the mirror map, FMA-PG is similar to the algorithm proposed in MDPO [34]. The difference between the two updates is that MDPO involves the advantage  $A^{\pi_t}$  instead of the  $Q^{\pi_t}$  term in Eq. (9).

However, the above formulation and MDPO have two main shortcomings. First, it involves  $p^{\pi}(a|s, \theta)$  which means that for each parametric update, either (i) the actions need to be resampled on-policy or (ii) the update involves an importance-sampling ratio  $p^{\pi}(a|s, \theta)/p^{\pi}(a|s, \theta_t)$  like in Eq. (9). This requires clipping the ratio for stability, and can result in potentially conservative updates [28]. With the mirror map as the negative entropy, the Bregman divergence is the *reverse* KL divergence, i.e.  $D_{\phi}(p^{\pi}(\cdot|s, \theta), p^{\pi}(\cdot|s, \theta_t)) = \text{KL}(p^{\pi}(\cdot|s, \theta) || p^{\pi}(\cdot|s, \theta_t))$ . The reverse KL divergence makes this objective *mode seeking*, in that the policy  $\pi$  might only capture a subset of the actions covered by  $\pi_t$ . Past works have addressed this issue either by adding entropy regularization [11, 29], or by simply reversing the KL, using the *forward* KL -  $\text{KL}(p^{\pi}(\cdot|s, \theta_t) || p^{\pi}(\cdot|s, \theta))$  [23]. However, using entropy regularization will result in a biased policy, whereas forward KL does not correspond to a valid Bregman divergence in  $p^{\pi}$  and can converge to a sub-optimal policy. We now show how

FMA-PG with the softmax representation addresses both these issues in a principled way, providing a theoretical justification to heuristics that are used to improve PG methods.

For the softmax functional representation considered in Section 4.2, we parameterize the logits as  $z^\pi(a, s, \theta)$ . Defining  $p^\pi(a|s, \theta) = z^\pi(a, s, \theta) / \sum_{a'} z^\pi(a', s, \theta)$  in Eq. (6) and noting that  $p^{\pi_t}(a|s) = p^\pi(a|s, \theta_t)$ , we obtain the following form of  $\ell_t^{\pi, \phi, \eta}(\theta)$ :

$$\ell_t^{\pi, \phi, \eta}(\theta) = E_{(s, a) \sim \mu^{\pi_t}} \left[ \left( A^{\pi_t}(s, a) + \frac{1}{\eta} \right) \log \frac{p^\pi(a|s, \theta)}{p^\pi(a|s, \theta_t)} \right] + C, \quad (10)$$

with  $C$  a constant independent of  $\theta$ . Unlike the formulation in Eq. (9), we see that Eq. (10) relies on the logarithm of the importance sampling ratios.

Moreover, Eq. (10) can be written as

$$\ell_t^{\pi, \phi, \eta} = \mathbb{E}_{s \sim d^{\pi_t}} \left[ \mathbb{E}_{a \sim p^{\pi_t}} \left( A^{\pi_t}(s, a) \log \frac{p^\pi(a|s, \theta)}{p^\pi(a|s, \theta_t)} \right) - \frac{1}{\eta} \text{KL}(p^\pi(\cdot|s, \theta_t) || p^\pi(\cdot|s, \theta)) \right]. \quad (11)$$

Comparing to Eq. (9), we observe that the KL divergence is in the *forward* direction and is *mode covering*. This naturally prevents a mode-collapse of the policy  $\pi$  and encourages exploration. We thus see that FMA-PG is able to recover an implementation heuristic (forward vs reverse KL) in a principled manner. Moreover, we can interpret Eq. (11) as an improved variant of TRPO.

**Comparison to TRPO:** Comparing Eq. (11) to the TRPO update [27],  $\arg \max_{\theta \in \mathbb{R}^d} \mathbb{E}_{(s, a) \sim \mu^{\pi_t}} \left[ A^{\pi_t}(s, a) \frac{p^\pi(a|s, \theta)}{p^\pi(a|s, \theta_t)} \right]$ , such that  $\mathbb{E}_{s \sim d^{\pi_t}} [\text{KL}(p^\pi(\cdot|s, \theta_t) || p^\pi(\cdot|s, \theta))] \leq \delta$ , we observe that Eq. (11) involves the logarithm of  $p^\pi$ . When the policy is modeled by a deep network with a final softmax layer, this leads to an objective concave in the last layer, which is in general easier to optimize than the original TRPO objective. Unlike TRPO, the proposed update enforces the proximity between policies via a regularization rather than a constraint. This modification has been recently found to be beneficial [21]. Moreover, the parameter  $\delta$  in TRPO is a hyper-parameter that needs to be tuned. In contrast, the regularization strength  $1/\eta$  in proposed update can be determined theoretically, as will be discussed in Section 6.

## 6 Theoretical guarantees

In this section, we will discuss how to set  $\eta$  according to the properties of  $J(\pi)$  for the direct and softmax functional representations, thus completely specifying the  $\ell_t^{\pi, \phi, \eta}(\theta)$  function.

FMA-PG obtains  $\pi_{t+1} = \pi(\theta_{t+1})$  through the (potentially approximate) maximization of  $\ell_t^{\pi, \phi, \eta}$  (Eq. (8)). Observe that  $J(\pi_t) = J(\pi(\theta_t)) = \ell_t^{\pi, \phi, \eta}(\theta_t)$ . A sufficient condition to guarantee that  $J(\pi_{t+1}) \geq J(\pi_t)$  is to make sure that  $\ell_t^{\pi, \phi, \eta}(\theta) \leq J(\pi(\theta))$  for all  $\theta$ . Indeed, if  $\ell_t$  lower bounds  $J$ , improving  $\ell_t$  i.e. ensuring that  $\ell_t^{\pi, \phi, \eta}(\theta)(\theta_{t+1}) \geq \ell_t^{\pi, \phi, \eta}(\theta)(\theta_t)$  leads to  $J(\pi_{t+1}) = J(\pi(\theta_{t+1})) \geq \ell_t^{\pi, \phi, \eta}(\theta_{t+1}) \geq \ell_t^{\pi, \phi, \eta}(\theta_t) = J(\pi(\theta_t)) = J(\pi_t)$ .

The following proposition shows that the values of  $\eta$  guaranteeing improvement are only dependent on properties of  $J$  and the mirror map in the function space and independent of the parameterization.

**Proposition 2** (Smoothness and improvement guarantees). *The surrogate function  $\ell_t^{\pi, \phi, \eta}$  is a lower bound of  $J$  if and only if  $J + \frac{1}{\eta} \phi$  is a convex function of  $\pi$ .*

The consequence of this proposition is that maximizing, even partially,  $\ell_t^{\pi, \phi, \eta}(\theta)$  and hence  $\ell_t^{\pi, \phi, \eta}(\theta)$  over  $\theta$ , starting from  $\theta = \theta_t$ , guarantees  $J(\pi_{t+1}) \geq J(\pi_t)$ .

The following proposition details how the direct and softmax functional representations satisfy the conditions of Proposition 2 and thus offer improvement guarantees:

**Proposition 3** (Improvement guarantees for direct and softmax representation). *Assume that the rewards are in  $[0, 1]$ . Then both the direct and the softmax representation accept values of  $\eta$  that guarantee improvement:*

- Direct:  $J \geq \ell_t^{p^\pi, \phi, \eta}$  with  $\phi$  the negative entropy and  $\eta \leq \frac{(1-\gamma)^3}{2\gamma|A|}$ .

- Softmax:  $J \geq \ell_t^{z^\pi, \phi_z, \eta_z}$  with  $\phi_z$  the exponential mirror map and  $\eta_z \leq 1 - \gamma$ .

Propositions 2 and 3 state that for specific values of  $\eta$ , any improvement to  $\ell_t$  (and hence  $\ell_t$ ) results in an improvement on the original objective. Moreover, these step-sizes only depend on the functional representation and the mirror map, and not on the particular parameterization chosen.

In order to show guaranteed improvement of  $\pi_{t+1} = \pi(\theta_{t+1})$ , we need to ensure that the parametric step-size  $\alpha$  is chosen according to the smoothness of  $\ell_t$ . With this, we obtain the following theorem:

**Theorem 1** (Guaranteed improvement for parametric update). *Assume that  $\ell_t$  is  $\beta$ -smooth w.r.t. the Euclidean norm and that  $\eta$  satisfies the condition of Proposition 2. Then, for any  $\alpha \leq 1/\beta$ , iteration  $t$  of Algorithm 1 guarantees  $J(\pi_{t+1}) \geq J(\pi_t)$  for any number  $m$  of inner loop updates.*

We see that by reparameterizing Eq. (3) into an unconstrained problem and solving it approximately with the correct choices of  $\eta$  and  $\alpha$  guarantees monotonic improvement in  $J(\pi)$ . For rewards in  $[0, 1]$ ,  $J(\pi)$  is upper-bounded by  $\frac{1}{1-\gamma}$ , and hence monotonic improvements to the policy results in convergence to a stationary point. We emphasize that the above result holds for any arbitrarily complicated policy parameterization. Hence, a successful PG method relies on two different notions of smoothness, one at the policy level (to set  $\eta$ ) and one at the parameter level (to set  $\alpha$ ). Note that Algorithm 1 and the corresponding theorem can be easily extended to handle stochastic parametric updates. This will guarantee that  $\mathbb{E}[J(\pi_{t+1})] \geq J(\pi_t)$  where the expectation is over the sampling in the parametric SGD steps. Similarly, both the algorithm and theoretical guarantee can be generalized to incorporate the relative smoothness of  $\ell_t(\theta)$  w.r.t. a general Bregman divergence.

Although we have used the same  $\eta$  for all states  $s$ , the updates in Eqs. (9) and (10) can accommodate a different step-size  $\eta(s)$  for each state. This is likely to yield tighter lower bounds and larger improvements in the inner loop. Determining such step-sizes is left for future work.

## 7 Experiments using FMA-PG with the softmax functional representation

While this work focuses on providing a general framework for designing PG methods, we explore the behaviour of FMA-PG with the softmax functional representation in three different settings: (i) A multi-armed bandit, where we compare it to the exponential weights algorithms (EXP3) [4] in Section 7.1; (ii) A small-scale RL environment where  $\ell$  in Eq. (8) can be maximized exactly in Appendix F; (iii) A larger-scale experiment on Mujoco, where we modify the update to make it similar to PPO [28], calling the resulting algorithm *sPPO*, in Section 7.2.

### 7.1 Multi-armed bandit

We compare EXP3, which corresponds to the single-state, tabular parameterization of FMA-PG with the direct representation and the negative entropy mirror map; to softmax EXP3 (*sEXP3*), which uses the softmax parameterization and the exponential mirror map. We do this in the context of a stochastic multi-armed bandit. However, we note that neither algorithm exploits the stochasticity in the rewards. For EXP3, we use the standard importance weighting procedure (denoted as IWEXP3 in the plots) as well as the loss-based variation [20] (denoted as LBIWEXP3). We swept over a range of step-sizes  $\eta$ , choosing the one which achieved the best average final regret for each algorithm over 50 runs (see Appendix E for details). Fig. 1 shows that *sEXP3* consistently achieves lower regret than both versions of EXP3, regardless of the number of arms (2, 10, 100) and the difficulty of the problem, as determined by the action gap.

### 7.2 Large-scale continuous control tasks

For the *sPPO* update, the  $\ell_t$  function in Algorithm 1 is given by:  $\ell_t^{\pi, \phi, \eta}(\theta) = \mathbb{E}_{(s, a) \sim \mu^{\pi_t}} \left[ A^{\pi_t}(s, a) \log \left( \text{clip} \left( \frac{p^\pi(a|s, \theta)}{p^{\pi_t}(a|s, \theta_t)}, \frac{1}{1+\epsilon}, 1+\epsilon \right) \right) \right]$  where the importance weight is clipped to the  $[\frac{1}{1+\epsilon}, 1+\epsilon]$  range, like PPO. We investigate the performance of *sPPO* on five standard continuous control environments from the OpenAI Gym suite [5]: Hopper-v1, Walker2d-v1, HalfCheetah-v1, Ant-v1, and Humanoid-v1. As a baseline, we use the PPO implementation from Andrychowicz et al. [3] with their standard configuration and all the hyperparameters set to the default values in Table 2 of Appendix C of [3]. We implement *sPPO* by adding a binary flag (`use_softmax`).

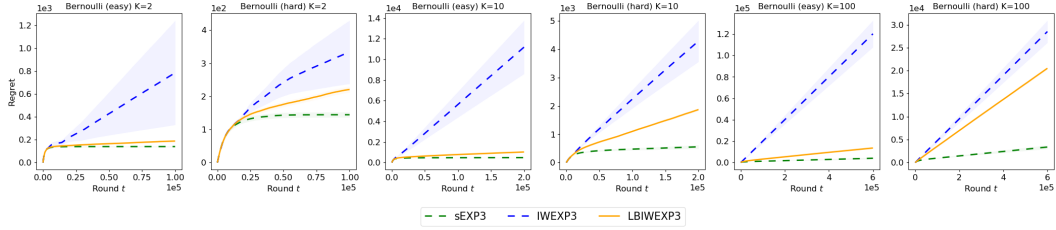


Figure 1: Comparing the average regret over 50 runs for two variants of EXP3 – with standard importance weights (IWEXP3) or loss-based importance weights (LBIWEXP3) to that of sEXP3. Both algorithms use a tuned step-size equal to 0.005. We observe that sEXP3 consistently achieves lower regret. See Appendix E for more results.

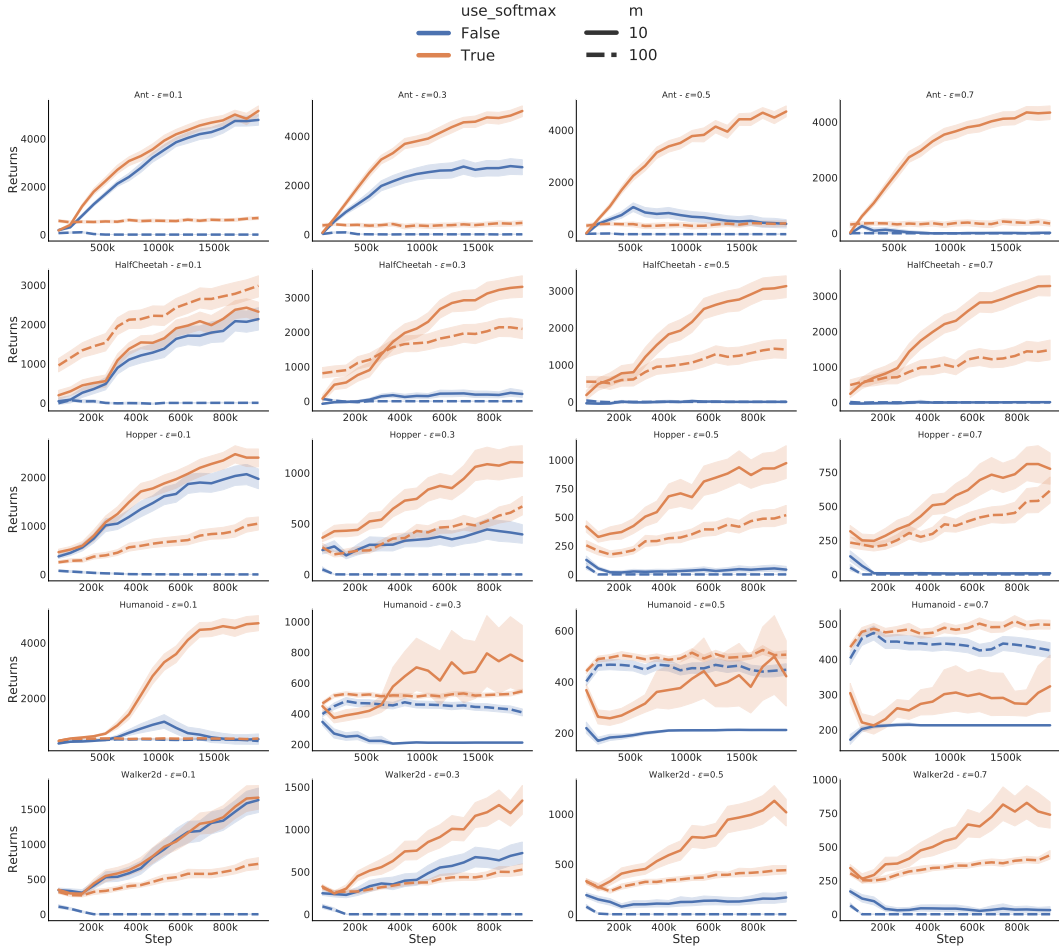


Figure 2: Average return and 95% confidence intervals (over 180 runs) for PPO and sPPO on 5 environments (rows) and for four different clipping values (columns). sPPO is more robust to large values of clipping, even more so when the number of updates in the inner loop grows (linestyle).

We investigate the differences between PPO and sPPO by training 180 different policies for each environment and all combinations of  $\text{use\_softmax} \in \{\text{True}, \text{False}\}$ ,  $m \in \{10, 100\}$  and the importance weight capping value  $\epsilon \in \{0.1, 0.3, 0.5, 0.7\}$  (a total compute of 1400 days with TPUv2). We evaluate each policy 18 times during training, using the action with largest probability rather than a sample. We compute the average return and 95% confidence intervals for each of the settings. The results are presented in Fig. 2, where we see that sPPO outperforms PPO across all environments. Furthermore, we see that the difference is more pronounced when the number of iterations  $m$  in the inner loop is increased (linestyles) or when less capping is used (columns). In the Appendix, we show additional results but with learning rate decay and gradient clipping disabled, two commonly used techniques to stabilize PPO training [9]. In this setting, sPPO only suffers a mild degradation while PPO fails completely, again confirming the additional robustness of sPPO compared to PPO.

## 8 Conclusion

In this paper, we proposed FMA-PG, a general framework to design computationally efficient policy gradient methods. By disentangling the functional representation of a policy from its parameterization, we unified different PG perspectives, recovering several existing algorithms and implementation heuristics in a principled manner. We also enabled the design of new, improved PG methods, as testified by the strong results of the softmax formulation in various settings. By using the appropriate theoretically-determined hyper-parameters, FMA-PG guarantees policy improvement (and hence convergence to a stationary point) for the resulting PG method, even with arbitrarily complex policy parameterizations and for arbitrary number of inner loop steps. We believe this to be of great interest as it allows the natural design of sample-efficient, off-policy methods. Our theoretical results assume the exact computation of the action-value and advantage functions, and are thus, limiting in practice. In the future, we aim to handle sampling errors and extend these results to the actor-critic framework. Furthermore, we hope to use the FMA-PG framework to develop other theoretically-principled PG methods.

## References

- [1] Abbas Abdolmaleki, Jost Tobias Springenberg, Yuval Tassa, Rémi Munos, Nicolas Heess, and Martin A. Riedmiller. Maximum a posteriori policy optimisation. In *International Conference on Learning Representations (ICLR)*, 2018.
- [2] Alekh Agarwal, Sham M. Kakade, Jason D. Lee, and Gaurav Mahajan. Optimality and approximation with policy gradient methods in Markov decision processes. In *Conference on Learning Theory (COLT)*, pages 64–66, 2020.
- [3] Marcin Andrychowicz, Anton Raichuk, Piotr Stanczyk, Manu Orsini, Sertan Girgin, Raphaël Marinier, Léonard Huszenot, Matthieu Geist, Olivier Pietquin, Marcin Michalski, et al. What matters for on-policy deep actor-critic methods? a largescale study. In *International conference on learning representations*, 2021.
- [4] Peter Auer, Nicolo Cesa-Bianchi, Yoav Freund, and Robert E Schapire. The nonstochastic multiarmed bandit problem. *SIAM journal on computing*, 32(1):48–77, 2002.
- [5] Greg Brockman, Vicki Cheung, Ludwig Pettersson, Jonas Schneider, John Schulman, Jie Tang, and Wojciech Zaremba. Openai gym. *arXiv preprint arXiv:1606.01540*, 2016.
- [6] Sébastien Bubeck. Convex optimization: Algorithms and complexity. *Foundations and Trends® in Machine Learning*, 8(3-4):231–357, 2015.
- [7] Shicong Cen, Chen Cheng, Yuxin Chen, Yuting Wei, and Yuejie Chi. Fast global convergence of natural policy gradient methods with entropy regularization. *arXiv preprint arXiv:2007.06558*, 2020.
- [8] Prafulla Dhariwal, Christopher Hesse, Oleg Klimov, Alex Nichol, Matthias Plappert, Alec Radford, John Schulman, Szymon Sidor, Yuhuai Wu, and Peter Zhokhov. Openai baselines. <https://github.com/openai/baselines>, 2017.

- [9] Logan Engstrom, Andrew Ilyas, Shibani Santurkar, Dimitris Tsipras, Firdaus Janoos, Larry Rudolph, and Aleksander Madry. Implementation matters in deep RL: A case study on PPO and TRPO. In *International conference on learning representations*, 2019.
- [10] Vincent Fran ois-Lavet, Peter Henderson, Riashat Islam, Marc G Bellemare, Joelle Pineau, et al. An introduction to deep reinforcement learning. *Foundations and Trends® in Machine Learning*, 11(3-4):219–354, 2018.
- [11] Matthieu Geist, Bruno Scherrer, and Olivier Pietquin. A theory of regularized Markov decision processes. In *International Conference on Machine Learning*, pages 2160–2169. PMLR, 2019.
- [12] Dibya Ghosh, Marlos C Machado, and Nicolas Le Roux. An operator view of policy gradient methods. *Advances in Neural Information Processing Systems*, 33, 2020.
- [13] Nicolas Heess, Gregory Wayne, David Silver, Timothy Lillicrap, Tom Erez, and Yuval Tassa. Learning continuous control policies by stochastic value gradients. In *Advances in Neural Information Processing Systems*, pages 2944–2952, 2015.
- [14] Rie Johnson and Tong Zhang. Guided learning of nonconvex models through successive functional gradient optimization. In *International Conference on Machine Learning*, pages 4921–4930. PMLR, 2020.
- [15] Sham Kakade. A natural policy gradient. In *NIPS*, volume 14, pages 1531–1538, 2001.
- [16] Sham Kakade and John Langford. Approximately optimal approximate reinforcement learning. In *International Conference on Machine Learning (ICML)*, pages 267–274, 2002.
- [17] Sham M Kakade. A natural policy gradient. In *Advances in neural information processing systems*, pages 1531–1538, 2002.
- [18] Sajad Khodadadian, Prakirt Raj Jhunjhunwala, Sushil Mahavir Varma, and Siva Theja Maguluri. On the linear convergence of natural policy gradient algorithm. *arXiv preprint arXiv:2105.01424*, 2021.
- [19] Vijay R Konda and John N Tsitsiklis. Actor-critic algorithms. In *Advances in neural information processing systems*, pages 1008–1014, 2000.
- [20] Tor Lattimore and Csaba Szepesv ri. *Bandit algorithms*. Cambridge University Press, 2020.
- [21] Nevena Lazi , Botao Hao, Yasin Abbasi-Yadkori, Dale Schuurmans, and Csaba Szepesv ri. Optimization issues in kl-constrained approximate policy iteration. *arXiv preprint arXiv:2102.06234*, 2021.
- [22] Haihao Lu, Robert M Freund, and Yurii Nesterov. Relatively smooth convex optimization by first-order methods, and applications. *SIAM Journal on Optimization*, 28(1):333–354, 2018.
- [23] Jincheng Mei, Chenjun Xiao, Ruitong Huang, Dale Schuurmans, and Martin M ller. On principled entropy exploration in policy optimization. In *IJCAI*, pages 3130–3136, 2019.
- [24] Jincheng Mei, Chenjun Xiao, Csaba Szepesvari, and Dale Schuurmans. On the global convergence rates of softmax policy gradient methods. In *International Conference on Machine Learning*, pages 6820–6829. PMLR, 2020.
- [25] Gergely Neu, Anders Jonsson, and Vicen  G mez. A unified view of entropy-regularized Markov decision processes. *CoRR*, abs/1705.07798, 2017.
- [26] Martin L. Puterman. *Markov Decision Processes: Discrete Stochastic Dynamic Programming*. John Wiley & Sons, Inc., USA, 1994.
- [27] John Schulman, Sergey Levine, Pieter Abbeel, Michael Jordan, and Philipp Moritz. Trust region policy optimization. In *International Conference on Machine Learning (ICML)*, pages 1889–1897, 2015.
- [28] John Schulman, Filip Wolski, Prafulla Dhariwal, Alec Radford, and Oleg Klimov. Proximal policy optimization algorithms. *CoRR*, abs/1707.06347, 2017.

- [29] Lior Shani, Yonathan Efroni, and Shie Mannor. Adaptive trust region policy optimization: Global convergence and faster rates for regularized mdps. In *Proceedings of the AAAI Conference on Artificial Intelligence*, volume 34, pages 5668–5675, 2020.
- [30] David Silver, Guy Lever, Nicolas Heess, Thomas Degris, Daan Wierstra, and Martin Riedmiller. Deterministic policy gradient algorithms. *Journal of Machine Learning Research*, 2014.
- [31] Richard S. Sutton and Andrew G. Barto. *Reinforcement Learning: An Introduction*. MIT Press, 2 edition, 2018.
- [32] Richard S Sutton, David A McAllester, Satinder P Singh, and Yishay Mansour. Policy gradient methods for reinforcement learning with function approximation. In *Advances in Neural Information Processing Systems (NeurIPS)*, pages 1057–1063, 2000.
- [33] Emanuel Todorov, Tom Erez, and Yuval Tassa. Mujoco: A physics engine for model-based control. In *2012 IEEE/RSJ International Conference on Intelligent Robots and Systems*, pages 5026–5033. IEEE, 2012.
- [34] Manan Tomar, Lior Shani, Yonathan Efroni, and Mohammad Ghavamzadeh. Mirror descent policy optimization. *arXiv preprint arXiv:2005.09814*, 2020.
- [35] Sharan Vaswani, Abbas Mehrabian, Audrey Durand, and Branislav Kveton. Old dog learns new tricks: Randomized ucb for bandit problems, 2020.
- [36] Ronald J Williams. Simple statistical gradient-following algorithms for connectionist reinforcement learning. *Machine learning*, 8(3-4):229–256, 1992.
- [37] Ronald J Williams and Jing Peng. Function optimization using connectionist reinforcement learning algorithms. *Connection Science*, 3(3):241–268, 1991.

---

# Supplementary material

---

## Organization of the Appendix

- A Handling stochastic value gradients
- B Proofs for Section 3
- C Proofs for Section 4
- D Proofs for Section 6
- E Experimental details in the bandit setting
- F Experiments in the tabular setting
- G Additional experiments on MuJoCo environments

## A Handling stochastic value gradients

Thus far we have worked with the original formulation of policy gradients where a policy is a distribution over actions given states. An alternative approach is that taken by stochastic value gradients [13], that rely on the reparametrization trick. In this case, a policy is not represented by a distribution over actions but rather by a set of actions. Formally, if  $\varepsilon$  are random variables drawn from a fixed distribution  $\nu$ , then policy  $\pi$  is a deterministic map from  $\mathcal{S} \times \nu \rightarrow \mathcal{A}$ . This corresponds to the functional representation of the policy. The action  $a$  chosen by  $\pi$  in state  $s$  (when fixing the random variable  $\varepsilon = \varepsilon$ ) is represented as  $\pi(s, \varepsilon)$  and

$$J(\pi) = \sum_s d^\pi(s) \int_\varepsilon \nu(\varepsilon) r(s, \pi(s, \varepsilon)) d\varepsilon \quad (12)$$

and Silver et al. [30] showed that  $\frac{\partial J(\pi)}{\partial \pi(s, \varepsilon)} = d^\pi(s) \nabla_a Q^\pi(s, a)|_{a=\pi(s, \varepsilon)}$ .

If the policy  $\pi$  is parameterized by model  $f$  with parameters  $\theta$ , then  $\pi(s, \varepsilon) = f(\theta, s, \varepsilon)$ . If  $f(\theta_t, \varepsilon)$  and  $f(\theta, \varepsilon)$  are  $S$ -dimensional vectors, then Eq. (3) is given as

$$\theta_{t+1} = \arg \min \mathbb{E}_{\varepsilon \sim \nu} \left[ - \sum_s d^{\pi_t}(s) f(\theta, s, \varepsilon) \nabla_a Q^{\pi_t}(s, a)|_{a=f(\theta_t, s, \varepsilon)} + \frac{1}{\eta} D_\phi(f(\theta, \varepsilon), f(\theta_t, \varepsilon)) \right]. \quad (13)$$

Similar to Sections 4.1 and 4.2, we will use a mirror map that decomposes across states. Specifically, we choose  $D_\phi(\pi, \mu) = \sum_{s \in \mathcal{S}} d^{\pi_t}(s) \|\pi(s) - \mu(s)\|^2$ . With this choice, Eq. (13) can be written as:

$$\theta_{t+1} = \arg \max \left[ \mathbb{E}_{s \sim d^{\pi_t}} \left[ \mathbb{E}_{\varepsilon \sim \nu} \left[ f(\theta, s, \varepsilon) \nabla_a Q^{\pi_t}(s, a)|_{a=f(\theta_t, s, \varepsilon)} - \frac{1}{\eta} \|f(\theta, \varepsilon) - f(\theta_t, \varepsilon)\|^2 \right] \right] \right] \quad (14)$$

This formulation is similar to Eq (15) of [30], with  $Q^{\pi_t}$  instead of  $Q^\pi$ . Additionally, while the authors justified the off-policy approach with an approximation, our formulation offers guarantees provided  $\eta$  satisfies the condition of Proposition 2.

## B Proofs for Section 3

**Proposition 1** (Operator consistency for the FMA update). *By defining the improvement and projection operators as the update and projection step of FMA, for the same mirror map (as in Eqs. (1) and (2)),  $\pi^*$  is a fixed point of  $\mathcal{P} \circ \mathcal{I}$ .*

*Proof.* Since  $\pi^*$  is the optimal policy, it is a stationary point of  $J(\pi)$ , implying that  $\nabla J(\pi^*) = 0$ . If we use the FMA update in Eq. (1) with  $\pi_t = \pi^*$ , then,

$$\pi_{t+1/2} = (\nabla \Phi)^{-1} (\nabla \phi(\pi^*) + \eta \nabla J(\pi^*)) \implies \pi_{t+1/2} = \pi^*.$$

For the projection in Eq. (2), using the above relation,

$$\pi_{t+1} = \arg \min_{\pi \in \Pi} D_\phi(\pi, \pi^*) \implies \forall \pi \in \Pi, D_\phi(\pi_{t+1}, \pi^*) \leq D_\phi(\pi, \pi^*)$$

Since  $\pi^* \in \Pi$ ,  $\min_{\pi \in \Pi} D_\phi(\pi, \pi^*) = 0$ ,  $\implies D_\phi(\pi_{t+1}, \pi^*) \leq 0$ . Since the Bregman divergence is non-negative,  $D_\phi(\pi_{t+1}, \pi^*) \implies \pi_{t+1} = \pi^*$ . The above relations imply that if  $\pi_t = \pi^*$ , the FMA update ensures that  $\pi_{t+1} = \pi^*$  and hence  $\pi^*$  is a fixed point of  $\mathcal{P} \circ \mathcal{I}$ .

□

## C Proofs for Section 4

In this section, we prove the equivalence of the formulations in terms of the logits and in terms of  $\log \pi$ .

**Lemma 1.** *Let*

$$\phi(z) = \frac{\sum_a \exp(z(a))}{\sum_a \exp(z'(a))} \quad (15)$$

$$p^\pi(a) = \frac{\exp(z(a))}{\sum_{a'} \exp(z(a'))}, \quad (16)$$

for some fixed  $z'$ . Then

$$D_\phi(z, z') = KL(p^{\pi'} || p^\pi) + \Delta \quad (17)$$

where  $p^\pi$  and  $p^{\pi'}$  use  $z$  and  $z'$  respectively,  $z'$  is the one used in the denominator of the mirror map, and  $\Delta \leq 0$  is independent of  $p^\pi$ .

*Proof.*

$$\begin{aligned} D_\phi(z, z') &= \frac{\sum_a \exp(z(a))}{\sum_a \exp(z'(a))} - \frac{\sum_a \exp(z'(a))}{\sum_a \exp(z'(a))} - \frac{\sum_a \exp(z'(a))(z(a) - z'(a))}{\sum_a \exp(z'(a))} \\ &= \frac{\sum_a \exp(z(a))}{\sum_a \exp(z'(a))} - 1 - \sum_a p^{\pi'}(a)(z(a) - z'(a)) \\ &= \frac{\sum_a \exp(z(a))}{\sum_a \exp(z'(a))} - \sum_a p^{\pi'}(a)(z(a) - \delta - z'(a) + \delta') - 1 - \sum_a p^{\pi'}(a)(\delta - \delta') , \end{aligned}$$

where the last equation is true for all  $\delta$  and all  $\delta'$ . By choosing

$$\begin{aligned} \delta &= \log \left( \sum_a \exp(z(a)) \right) \\ \delta' &= \log \left( \sum_a \exp(z'(a)) \right) , \end{aligned}$$

we have

$$z(a) - \delta = \log p^\pi(a) ,$$

and

$$\begin{aligned} D_\phi(z, z') &= \exp(\delta - \delta') - \sum_a p^{\pi'}(a) \log \frac{p^\pi(a)}{p^{\pi'}(a)} - 1 + \delta' - \delta \\ &= KL(p^{\pi'} || p^\pi) + \exp(\delta - \delta') - 1 + \delta' - \delta . \end{aligned}$$

Shifting all values of  $z$  by the same amount affects  $\delta$  but not  $p^\pi$  because of the normalization. Hence,  $\exp(\delta - \delta') - 1 + \delta' - \delta$  is independent of  $p^\pi$ .

Finally, we use that  $\exp(x) - 1 - x \geq 0$  for all  $x$  with  $x = \delta - \delta'$  to conclude the proof. □

**Proposition 4.**

$$\ell_t^{z^\pi, \phi, \eta}(\theta) = J(\pi_t) + E_{(s, a) \sim \mu^{\pi_t}} \left( A^{\pi_t}(s, a) + \frac{1}{\eta} \right) \log \frac{p^\pi(a|s, \theta)}{p^{\pi_t}(a|s, \theta)} - \Delta, \quad (18)$$

with  $\Delta \leq 0$  a constant independent of  $\pi$ .

*Proof.* Because  $\sum_a p^{\pi_t}(a|s) A^{\pi_t}(s, a) = 0$ , we can shift all values of  $z$  by a term that does not depend on  $a$  without changing the sum, in particular by  $\log(\sum_{a'} \exp(z^\pi(a', s|\theta)))$ . Thus,

$$\begin{aligned} \ell_t^{z^\pi, \phi, \eta}(\theta) &= J(\pi_t) + E_{(s, a) \sim \mu^{\pi_t}} A^{\pi_t}(s, a) \left( z^\pi(a, s|\theta) - \log \left( \sum_{a'} \exp(z^\pi(a', s|\theta)) \right) \right) \\ &\quad - \frac{1}{\eta} \sum_s d^{\pi_t}(s) D_{\phi_z}(z^\pi(\cdot, s|\theta), z^\pi(\cdot, s, \theta_t)) \\ &= J(\pi_t) + E_{(s, a) \sim \mu^{\pi_t}} A^{\pi_t}(s, a) \log p^\pi(a|s, \theta) - \frac{1}{\eta} \sum_s d^{\pi_t}(s) D_{\phi_z}(z^\pi(\cdot, s|\theta), z^\pi(\cdot, s|\theta_t)). \end{aligned}$$

Using Lemma 1, we have

$$D_{\phi_z}(z^\pi(\cdot, s|\theta), z^\pi(\cdot, s|\theta_t)) = \sum_s d^{\pi_t}(s) \left( KL(p^{\pi'}(\cdot|s) || p^\pi(\cdot|s)) + \exp(\delta(s) - \delta'(s)) - 1 + \delta' - \delta \right),$$

for some  $\delta$  and  $\delta'$  independent of  $p^\pi$ .

Noting that

$$KL(p^{\pi'}(\cdot|s) || p^\pi(\cdot|s)) = \sum_a p^{\pi_t}(a|s) \log \frac{p^\pi(a|s)}{p^{\pi_t}(a|s)},$$

$$\ell_t^{z^\pi, \phi, \eta}(\theta) = J(\pi_t) + E_{(s, a) \sim \mu^{\pi_t}} \left( A^{\pi_t}(s, a) + \frac{1}{\eta} \right) \log \frac{p^\pi(a|s, \theta)}{p^{\pi_t}(a|s, \theta)} - \Delta,$$

with  $\Delta \leq 0$  independent of  $p^\pi$ . This concludes the proof.  $\square$

## D Proofs for Section 6

**Proposition 2** (Smoothness and improvement guarantees). *The surrogate function  $\ell_t^{\pi, \phi, \eta}$  is a lower bound of  $J$  if and only if  $J + \frac{1}{\eta}\phi$  is a convex function of  $\pi$ .*

*Proof.*

$$\begin{aligned} J(\pi) - \ell_t^{\pi, \phi, \eta}(\pi) &= J(\pi) - J(\pi_t) - \langle \pi - \pi_t, \nabla_\pi J(\pi_t) \rangle + \frac{1}{\eta} D_\phi(\pi, \pi_t) \\ &= J(\pi) - J(\pi_t) - \langle \pi - \pi_t, \nabla_\pi J(\pi_t) \rangle + \frac{1}{\eta} (\phi(\pi) - \phi(\pi_t) - \langle \nabla_\pi \phi(\pi_t), \pi - \pi_t \rangle) \\ &= \left( J + \frac{1}{\eta} \phi \right) (\pi) - \left( J + \frac{1}{\eta} \phi \right) (\pi_t) - \langle \pi - \pi_t, \nabla_\pi \left( J + \frac{1}{\eta} \phi \right) (\pi_t) \rangle. \end{aligned}$$

The last equation is positive for all  $\pi$  and all  $\pi_t$  if and only if  $J + \frac{1}{\eta}\phi$  is convex.  $\square$

To prove the value of  $\eta$  guaranteeing improvement for the softmax parameterization, we first need to extend a lower bound result from Ghosh et al. [12]:

**Proposition 5.** *Let us assume that the rewards are lower bounded by  $-c$  for some  $c \in \mathbb{R}$ . Then we have*

$$J(\pi) \geq J(\pi_t) + E_{(s, a) \sim \mu^{\pi_t}} \left[ \left( Q^{\pi_t}(s, a) + \frac{c}{1-\gamma} \right) \log \frac{p^\pi(a|s)}{p^{\pi_t}(a|s)} \right]. \quad (19)$$

*Proof.* Let us define the function  $J_\nu$  for a policy  $\nu$  as

$$J_\nu(\pi) = \sum_{h=0}^{+\infty} \gamma^h \int_{\tau_h} (r(s_h, a_h) + c) \left( 1 + \log \frac{\pi_h(\tau_h)}{\nu_h(\tau_h)} \right) \nu_h(\tau_h) d\tau_h - \frac{c}{1-\gamma} ,$$

where  $\tau_h$  is a trajectory of length  $h$  that is a prefix of a full trajectory  $\tau$  and  $\pi_h$  is the policy restricted to trajectories of length  $h$ . We first show that it satisfies  $J_\nu(\pi) \leq J(\pi)$  for any  $\nu$  and any  $\pi$  such that the support of  $\nu$  covers that of  $\pi$ .

Indeed, we can rewrite

$$\begin{aligned} J(\pi) &= \int_{\tau} \left( R(\tau) + \frac{c}{1-\gamma} \right) \pi(\tau) d\tau - \frac{c}{1-\gamma} \\ &= \int_{\tau} \left( \sum_h \gamma^h (r(a_h, s_h) + c) \right) \pi(\tau) d\tau - \frac{c}{1-\gamma} \quad (\text{using } \sum_h \gamma^h c = c/(1-\gamma)) \\ &= \sum_h \gamma^h \int_{\tau_h} (r(a_h, s_h) + c) \pi_h(\tau_h) d\tau_h - \frac{c}{1-\gamma} , \end{aligned}$$

where the last line is obtained by marginalizing over steps  $h+1, \dots, +\infty$  for all  $h$  and all trajectories  $\tau$ . Because  $r(a_h, s_h) + c$  is positive, as the rewards are lower bounded by  $-c$ , we have

$$\begin{aligned} J(\pi) &= \sum_h \gamma^h \int_{\tau_h} (r(a_h, s_h) + c) \frac{\pi_h(\tau_h)}{\nu_h(\tau_h)} \nu_h(\tau_h) d\tau_h - \frac{c}{1-\gamma} \\ &\geq \sum_h \gamma^h \int_{\tau_h} (r(a_h, s_h) + c) \left( 1 + \log \frac{\pi_h(\tau_h)}{\nu_h(\tau_h)} \right) \nu_h(\tau_h) d\tau_h - \frac{c}{1-\gamma} \\ &\quad (\text{using } x \geq 1 + \log x) \\ &= J_\nu(\pi) . \end{aligned}$$

Let us denote  $J_\nu^{SA}$  the right-hand side of Eq. (19), i.e.:

$$J_\nu^{SA}(\pi) = J(\nu) + E_{(s,a) \sim \mu^\nu} \left[ \left( Q^\nu(s, a) + \frac{c}{1-\gamma} \right) \log \frac{p^\pi(a|s)}{p^\nu(a|s)} \right] .$$

We now prove that  $J_\nu$  has the same gradient as  $J_\nu^{SA}$ :

$$\begin{aligned} \nabla_\theta J_\nu(\pi) &= \nabla_\theta \left( \sum_h \gamma^h \int_{\tau_h} (r(a_h, s_h) + c) \left( 1 + \log \frac{\pi_h(\tau_h)}{\nu_h(\tau_h)} \right) \nu_h(\tau_h) d\tau_h \right) \\ &= \nabla_\theta \left( \sum_h \gamma^h \int_{\tau_h} (r(a_h, s_h) + c) \log \pi_h(\tau_h) \nu_h(\tau_h) \right) d\tau_h \\ &= \sum_h \gamma^h \int_{\tau_h} (r(a_h, s_h) + c) \nabla_\theta \log \pi_h(\tau_h) \nu_h(\tau_h) d\tau_h , \end{aligned}$$

where all terms independent of  $\theta$  were moved outside of the gradient. As the log probability of a trajectory decomposes into a sum of the probabilities of actions given states and of the transition probabilities, and as the latter are independent of  $\theta$ , we get

$$\begin{aligned} \nabla_\theta J_\nu(\pi) &= \sum_h \gamma^h \int_{\tau_h} (r(a_h, s_h) + c) \nabla_\theta \log \pi_h(\tau_h) \nu_h(\tau_h) d\tau_h \\ &= \sum_h \gamma^h \int_{\tau_h} (r(a_h, s_h) + c) \left( \sum_{h'} \nabla_\theta \log p^\pi(a_{h'}|s_{h'}) \right) \nu_h(\tau_h) d\tau_h \\ &= \int_{\tau} \sum_{h'} \nabla_\theta \log p^\pi(a_{h'}|s_{h'}) \left( \sum_{h=h'}^{+\infty} \gamma^h (r(a_h, s_h) + c) \right) \nu(\tau) d\tau . \end{aligned}$$

But

$$\begin{aligned} \sum_{h=h'}^{+\infty} \gamma^h (r(a_h, s_h) + c) &= \gamma^{h'} \left( Q^\nu(s, a) + \frac{c}{1-\gamma} \right) \\ \int_{\tau} \nu(\tau) d\tau 1_{a_{h'}=a} 1_{s_{h'}=s} &= d_\nu^{h'}(s) \nu(a|s), \end{aligned}$$

with  $d_\nu^{h'}(s)$  the undiscounted probability of reaching state  $s$  at timestep  $h'$ . Hence, we have

$$\begin{aligned} \nabla_\theta J_\nu(\pi) &= \int_{\tau} \sum_{h'} \nabla_\theta \log p^\pi(a_{h'}|s_{h'}) \left( \sum_{h=h'}^{+\infty} \gamma^h (r(a_h, s_h) + c) \right) \nu(\tau) d\tau \\ &= \sum_{h'} \sum_s \sum_a \nabla_\theta \log p^\pi(a|s) d_\nu^{h'}(s) \nu(a|s) \gamma^{h'} \left( Q^\nu(s, a) + \frac{c}{1-\gamma} \right) \\ &= \sum_{h'} \gamma^{h'} \sum_s d_\nu^{h'}(s) \sum_a \nabla_\theta \log p^\pi(a|s) \nu(a|s) \left( Q^\nu(s, a) + \frac{c}{1-\gamma} \right) \\ &= \sum_s d^\nu(s) \sum_a \left( Q^\nu(s, a) + \frac{c}{1-\gamma} \right) \nu(a|s) \nabla_\theta \log p^\pi(a|s) \\ &= \nabla_\theta \left( \sum_s d^\nu(s) \sum_a \left( Q^\nu(s, a) + \frac{c}{1-\gamma} \right) \nu(a|s) \log p^\pi(a|s) \right) \\ &= \nabla_\theta \left( J(\nu) + E_{(s,a) \sim \mu^\nu} \left[ \left( Q^\nu(s, a) + \frac{c}{1-\gamma} \right) \log \frac{p^\pi(a|s)}{p^\nu(a|s)} \right] \right) \\ &= \nabla_\theta J_\nu^{SA}(\pi), \end{aligned}$$

with  $d^\nu(s)$  the unnormalized probability of  $s$  under the *discounted* stationary distribution.

Because  $J_\nu$  and  $J_\nu^{SA}$  have the same gradient, they differ by a constant, i.e.  $J_\nu^{SA} = J_\nu + C$  for some  $C$ . But we also know that  $J_\nu(\nu) = J(\nu)$ , which means that

$$\begin{aligned} C &= J_\nu^{SA}(\nu) - J_\nu(\nu) \\ &= J_\nu^{SA}(\nu) - J(\nu) \\ &= E_{(s,a) \sim \mu^\nu} \left[ \left( Q^\nu(s, a) + \frac{c}{1-\gamma} \right) \log \frac{p^\nu(a|s)}{p^\nu(a|s)} \right] \\ &= 0. \end{aligned}$$

Hence,  $J_\nu = J_\nu^{SA}$  and, becomes  $J_\nu$  is a lower bound of  $J$ , we have

$$J(\pi) \geq J(\nu) + \sum_s d^\nu(s) \sum_a \left( Q^\nu(s, a) + \frac{c}{1-\gamma} \right) p^\nu(a|s) \log \frac{p^\pi(a|s)}{p^\nu(a|s)}. \quad (20)$$

Setting  $\nu = \pi_t$  concludes the proof.  $\square$

**Proposition 3** (Improvement guarantees for direct and softmax representation). *Assume that the rewards are in  $[0, 1]$ . Then both the direct and the softmax representation accept values of  $\eta$  that guarantee improvement:*

- Direct:  $J \geq \ell_t^{p^\pi, \phi, \eta}$  with  $\phi$  the negative entropy and  $\eta \leq \frac{(1-\gamma)^3}{2\gamma|A|}$ .
- Softmax:  $J \geq \ell_t^{z^\pi, \phi_z, \eta_z}$  with  $\phi_z$  the exponential mirror map and  $\eta_z \leq 1 - \gamma$ .

*Proof.* Agarwal et al. [2] show that, when using the direct parameterization,  $J$  is  $\left(\frac{2\gamma|A|}{(1-\gamma)^3}\right)$ -smooth w.r.t. the Euclidean distance. By using the properties of relative smoothness [22], if the mirror map  $\phi$  is  $\mu$ -strongly convex w.r.t. Euclidean distance, then  $J$  is  $L$ -smooth with  $L = (2\gamma|A|/(1-\gamma)^3)\mu$ . Using

the fact that negative entropy is 1-strongly convex w.r.t. the 1-norm, we can set  $\eta = (1-\gamma)^3/2\gamma|A|$  in Eq. (4).

We now prove the result for the softmax parameterization. Assume

$$\eta = \frac{1-\gamma}{r_m - r_l} . \quad (21)$$

We know from Proposition 4 that

$$\ell_t^{z^\pi, \phi, \eta}(\theta) \leq J(\pi_t) + E_{(s, a) \sim \mu^{\pi_t}} \left( A^{\pi_t}(s, a) + \frac{1}{\eta} \right) \log \frac{p^\pi(a|s, \theta)}{p^{\pi_t}(a|s, \theta)} .$$

Since the rewards are between  $r_l$  and  $r_m$ , we have

$$\begin{aligned} \ell_t^{z^\pi, \phi, \eta}(\pi) &\leq J(\pi_t) + E_{(s, a) \sim \mu^{\pi_t}} \left[ \left( A^{\pi_t}(s, a) + \frac{1}{\eta} \right) \log \frac{p^\pi(a|s)}{p^{\pi_t}(a|s)} \right] \\ &= J(\pi_t) + E_{(s, a) \sim \mu^{\pi_t}} \left[ \left( A^{\pi_t}(s, a) + \frac{r_m - r_l}{1-\gamma} \right) \log \frac{p^\pi(a|s)}{p^{\pi_t}(a|s)} \right] \\ &= J(\pi_t) + E_{(s, a) \sim \mu^{\pi_t}} \left[ \left( A^{\pi_t}(s, a) + V^{\pi_t}(s) + \left( \frac{r_m}{1-\gamma} - V^{\pi_t}(s) \right) - \frac{r_l}{1-\gamma} \right) \log \frac{p^\pi(a|s)}{p^{\pi_t}(a|s)} \right] \\ &= J(\pi_t) + E_{(s, a) \sim \mu^{\pi_t}} \left[ \left( Q^{\pi_t}(s, a) - \frac{r_l}{1-\gamma} \right) \log \frac{p^\pi(a|s)}{p^{\pi_t}(a|s)} \right] \\ &\quad - E_{s \sim d^{\pi_t}} \left[ \left( \frac{r_m}{1-\gamma} - V^{\pi_t}(s) \right) KL(p^{\pi_t}(\cdot|s) || p^\pi(\cdot|s)) \right] . \end{aligned}$$

The last term on the RHS of the last equation is negative. Indeed, because the rewards are less than  $r_m$ , the value functions are less than  $r_m/(1-\gamma)$  and  $r_m/(1-\gamma) - V^{\pi_t}(s)$  is positive. As the KL divergences are positive, the product of the two is positive and the whole term is negative because of the minus term. Thus, we have

$$\begin{aligned} \ell_t^{z^\pi, \phi, \eta}(\pi) &\leq J(\pi_t) + E_{(s, a) \sim \mu^{\pi_t}} \left[ \left( Q^{\pi_t}(s, a) - \frac{r_l}{1-\gamma} \right) \log \frac{p^\pi(a|s)}{p^{\pi_t}(a|s)} \right] \\ &\leq J(\pi) . \end{aligned} \quad (\text{by Proposition 5})$$

Hence, choosing  $\eta = \frac{1-\gamma}{r_m - r_l}$  leads to an improvement guarantee. Because our rewards are bounded between 0 and 1, setting  $r_m = 1$  and  $r_l = 0$  gives  $\eta = 1 - \gamma$ . This concludes the proof.  $\square$

**Theorem 1** (Guaranteed improvement for parametric update). *Assume that  $\ell_t$  is  $\beta$ -smooth w.r.t. the Euclidean norm and that  $\eta$  satisfies the condition of Proposition 2. Then, for any  $\alpha \leq 1/\beta$ , iteration  $t$  of Algorithm 1 guarantees  $J(\pi_{t+1}) \geq J(\pi_t)$  for any number  $m$  of inner loop updates.*

*Proof.* Using the update in Algorithm 1 with  $\alpha = \frac{1}{\beta}$  and the  $\beta$ -smoothness of  $\ell_t(\omega)$ , for all  $k \in [m-1]$ ,

$$\ell_t(\omega_{k+1}) \geq \ell_t(\omega_k) + \frac{1}{2\beta} \|\nabla \ell_t(\omega_k)\|^2$$

After  $m$  steps,

$$\ell_t(\omega_m) \geq \ell_t(\omega_0) + \frac{1}{2\beta} \sum_{k=0}^{m-1} \|\nabla \ell_t(\omega_k)\|^2$$

Since  $\theta_{t+1} = \omega_m$  and  $\omega_0 = \theta_t$  in Algorithm 1,

$$\implies \ell_t(\theta_{t+1}) \geq \ell_t(\theta_t) + \frac{1}{2\beta} \|\nabla \ell_t(\theta_t)\|^2 + \sum_{k=1}^{m-1} \|\nabla \ell_t(\omega_k)\|^2$$

Note that  $J(\pi_t) = \ell_t(\theta_t)$  and if  $\eta$  satisfies Proposition 2, then  $J(\pi_{t+1}) \geq \ell_t(\theta_{t+1})$ . Using these relations,

$$J(\pi_{t+1}) \geq J(\pi_t) + \underbrace{\frac{1}{2\beta} \|\nabla \ell_t(\theta_t)\|^2 + \sum_{k=1}^{m-1} \|\nabla \ell_t(\omega_k)\|^2}_{+ve} \implies J(\pi_{t+1}) \geq J(\pi_t).$$

□

## E Experimental details in the bandit setting

In this section, we detail the experimental setup for the bandit experiments in Section 7.1.

We consider different  $K$ -armed Bernoulli bandit problems. For sEXP3, we specialising the update rule in Eq. (6) to this multi-armed bandit case yielding:  $p^{\pi_{t+1}}(a) = p^{\pi_t}(a)(1 + \eta A^{\pi_t}(a))$ , where  $\eta$  needs to be chosen such that the probabilities are always positive. However, the computing the advantage either requires knowledge of the rewards of all arms, or an estimate thereof. Since EXP3 is an adversarial bandit algorithm and does not exploit the stochasticity in the rewards, to ensure a fair comparison, we cannot use such an estimate and thus replace the advantage with the immediate reward, leading to the final sEXP3 update:

$$p^{\pi_{t+1}}(a) = p^{\pi_t}(a)(1 + \eta \hat{r}_t(a)),$$

where  $\hat{r}_t(a)$  an estimator of the reward  $r_t(a)$  obtained at round  $t$ .

For sEXP3, if  $A_t$  is the action taken at round  $t$ , then we use the importance weighted estimator  $\hat{r}_t(a) = \mathbb{I}\{A_t = 1\}r_t(a)/\pi_t(a)$ . For EXP3, we consider both the standard importance weighted estimator (referred to as IWEXP3 in the plots) and the loss based importance weighted estimator (referred to as LBIWEXP3 in the plots) for which  $\hat{r}_t(a) = \mathbb{I}\{A_t = 1\}(1 - r_t(a))/\pi_t(a)$ .

Before describing our experimental setup, we emphasize that there are two different sources of randomness in our experiments. First, we have the *environment seed* that controls the mean rewards in the bandit problem. Considering different environment seeds guarantees that our results are not specific to a particular choice of the rewards. Given a specific bandit problem, since EXP3 and sEXP3 are randomized bandit algorithms, there is a stochasticity in the actions chosen. We can use different *agent seeds* to control the algorithm randomness.

Following the evaluation protocol of [35], we consider two classes of bandits with different action gaps (difference in the mean rewards) – hard instances ( $\Delta = 0.5$ ) and easy instances ( $\Delta = 0.1$ ). The mean vector defining a Bernoulli bandit is then sampled entry wise (for each arm) from  $\mathcal{U}(0.5 - \Delta/2, 0.5 + \Delta/2)$ . To obtain the plot in Section 7.1, we run the experiment for 50 different environment seeds and one agent seed. We evaluated the three algorithms for Bernoulli bandits with  $K \in \{2, 10, 100\}$  arms and the difficulty of the problem, as determined by the action gap. For each algorithm, we set the step-size via a grid search over  $\eta \in \{0.5, 0.05, 0.005, 0.0005, 0.00005\}$ . The plot shows the regret corresponding to the step-size with lowest final average regret.

## F Experiments in the tabular setting

We compare Mirror Descent Policy optimization (MDPO), which corresponds to the tabular parametrization of FMA-PG with direct representation and the weighted negative entropy as a mirror map, to FMA-PG with the softmax representation and the weighted exponential mirror map. We slightly abuse naming convention and denote this latter algorithm softmax PPO (*sPPO*).

We run these experiments on a variation of the Cliff MDP [31]. The Cliff MDP is a  $7 \times 7$  navigation problem, with a subset of special states, the cliff states, nearby the absorbing goal state. When the agent reaches a cliff state, it receives a large negative reward and is teleported back to the starting state. At the absorbing state, the agent receives a positive reward (+1) forever. In this MDP, the optimal policy is to move close to the Cliff, and a “safer” but suboptimal policy is to transit away from the Cliff.

We can see in Fig. 3 that sPPO slightly outperforms MDPO for  $\eta = 0.03$ . However, for larger step-sizes, sPPO prefers the “safer” but suboptimal route while MDPO converges to the optimal policy.

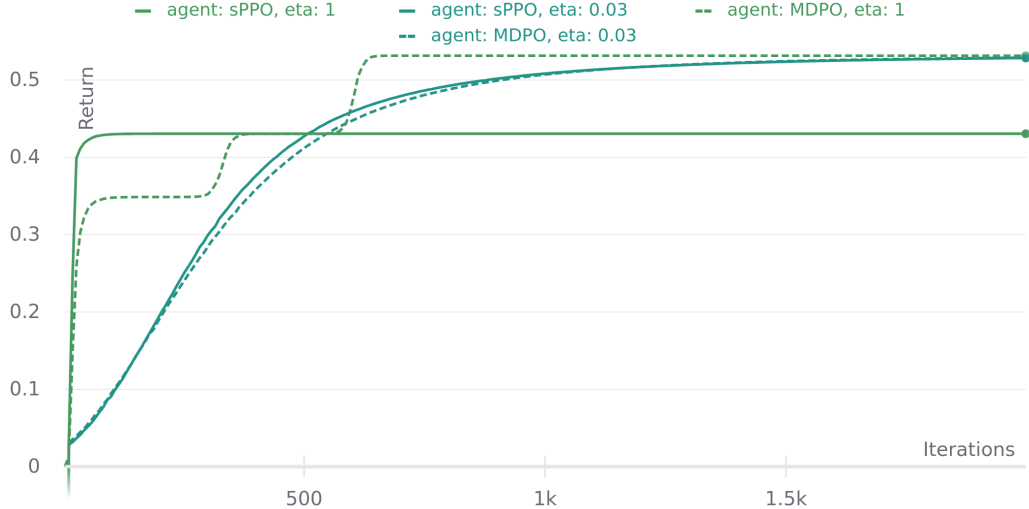


Figure 3: Expected return of MDPO and sPPO on the Cliff environment. MDPO outperforms sPPO on this environment. While sPPO with a large learning rate has an early increase in return, it gets stuck in a suboptimal solution (the “safe” path). sPPO with a smaller learning rate reaches the optimal solution, but much slower than MDPO.

Our intuition for this behaviour is that Cliff is an “easy” problem, in the sense that an aggressive approach will generally work better. In that case, replacing the reverse KL with the forward KL is unlikely to have a large impact. However, using a large stepsize with sPPO will lead to the probability of some actions being exactly 0 (see paragraph “Tabular parameterization” at the end of Section 4.2) and these actions will never be selected again. If one of these actions belongs to the optimal policy, then sPPO will only converge to a suboptimal policy, which is what happens with  $\eta = 1$ .

Given the discrepancy between these results and those obtained on both bandits and MuJoCo, we posit that sPPO’s strength lies when there is uncertainty that needs to be maintained, whether it’s due to the stochasticity or to function approximation.

## G Additional experiments on MuJoCo environments

In this section, we present results on a series of MuJoCo environments where learning rate decay and gradient clipping have *not* been applied. Fig. 4 shows that, while sPPO (in orange) still learns something, PPO is unable to make progress, regardless of the capping ( $\epsilon$ ) and the number of inner loop steps ( $m$ ), further reinforcing our intuition that the softmax parameterization leads to a more robust optimization.

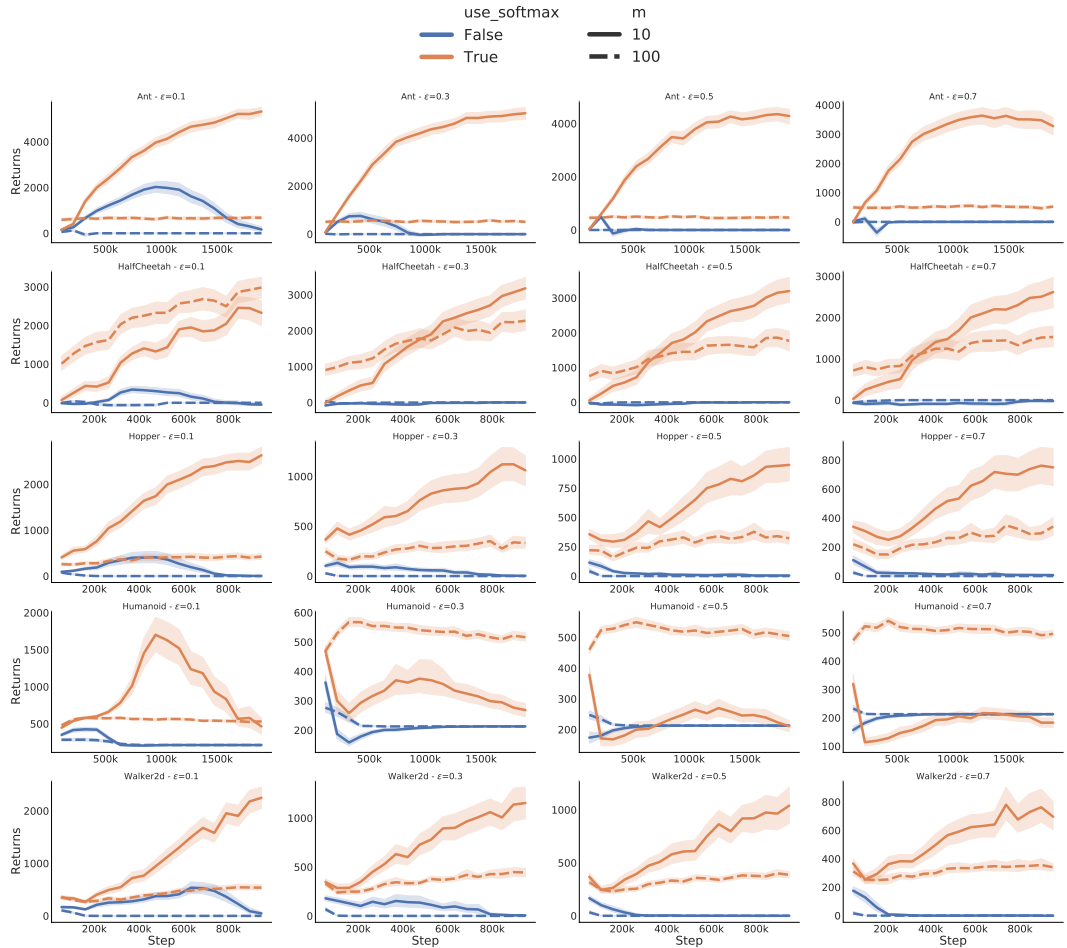


Figure 4: Average discounted return and 95% confidence interval (over 180 runs) for PPO and softmax PPO on 4 environments (*env* - rows) and for four different clipping strengths (*epsilon* - columns). We see that sPPO is more robust to large values of clipping, even more so when the number of updates in the inner loop grows (linestyle).